Water-Soluble Complexes Formed by Sodium Poly(4-styrenesulfonate) and a Poly(2-vinylpyridinium)-*block*-poly(ethyleneoxide) Copolymer

Jean-François Gohy,[†,‡] Sunil K. Varshney,[§] Sayed Antoun,[†] and Robert Jérôme*[,†]

Center for Education and Research on Macromolecules (CERM),Institute of Chemistry B6, University of Liège, Sart-Tilman, B-4000 Liège, Belgium; and Polymer Source, 771 Lajoie Street, Dorval, PQ H9P 1G7, Canada

Received July 6, 2000; Revised Manuscript Received October 5, 2000

ABSTRACT: Formation of interpolyelectrolyte complexes (IPEC) between sodium poly(4-styrenesulfonate) ($PSSO_3Na$) and a diblock copolymer consisting of a protonated poly(2-vinylpyridine) (P2VP) block and a neutral poly(ethylene oxide) (PEO) one was investigated in water. The main experimental variables were the molecular weight (MW) of the $PSSO_3Na$ polyanion, the molar ratio of the cationic and anionic species (i.e., the stoichiometry of the complex), and the pH of the aqueous solution. It was observed that (i) the interpolyelectrolyte complexes self-assemble at least at low pH into the core of monodisperse spherical micelles surrounded by a corona of PEO blocks and possibly of uncomplexed $PSSO_3Na$ segments, (ii) their stability depends on the pH in relation to the degree of protonation of the P2VP block, whatever the MW of the $PSSO_3Na$ polyanion and the cation/anion stoichiometry, (iii) the complexes are dissociated above a critical pH and are salt-sensitive, falling apart above a critical salt concentration, and (iv) a cooperative mechanism operates, which is completely reversible.

Introduction

Steadily increasing attention is paid nowadays to water-soluble polymeric surfactants not only for their supramolecular organization in water but also because of potential applications in quite different fields, such as pigment stabilization in water-born coatings[1] and drug delivery systems.[2] These polymeric amphiphiles are usually diblock copolymers consisting of an insoluble block whose supramolecular aggregation forms a dense core and a soluble block which extends out into the solvent and forms the solvated corona of micelles.[3]

Micelles of various shape have been reported, ranging from spherical micelles[4] to vesicles[5−8] and complex superaggregates.[9,10] In the past decade, most attention was paid to micellization of diblock copolymers in water. However, the diblock used and, in particular, the composition were such that direct dissolution in water was a problem and required the temporary use of an organic cosolvent, such as methanol and tetrahydrofuran, for the preparation of stable and well-defined micelles.[11]

A more straightforward way to prepare polymeric micelles in water is to consider polymeric amphiphiles with two water-soluble blocks, at least in some pH range, which spontaneously aggregate upon an appropriate change of pH, one block being then insoluble in water.[12,13] This strategy was successfully used by Webber et al. in the case of P2VP-*b*-PEO copolymers, which formed unimers at low pH and micelles at pH higher than 4.8.[14] Recently Armes et al. synthesized poly(2-diethylaminoethyl methacrylate)-*block*-poly(2-dimethylaminoethyl methacrylate) copolymers, which formed micelles in water above a critical pH, as result of a slight difference in the pK_a's of the two aminated blocks.[12,15]

In addition to the amphiphilic block copolymers, interpolyelectrolyte complexes (IPEC) are receiving a special attention.[16,17] They are formed as result of electrostatic interactions between oppositely charged polyions. The properties of these complexes strongly depend on their composition. Nonstoichiometric complexes, thus containing an excess of one charged constitutive component, have a net charge and are usually water-soluble. The stoichiometric complexes, being electroneutral, usually precipitate from the aqueous solution.

IPEC have the potential to form micellar aggregates.[19−23] Indeed, micelles are small droplets of a new phase that has been arrested in its growth because part of the constituent molecule does not participate to phase separation and remains in contact with the solvent. In the case of IPEC, the electrostatic interaction of oppositely charged polymers, is at the origin of phase separation. This strategy has been recently used by Kataoka et al., who prepared monodisperse spherical aggregates merely by mixing poly(ethylene oxide)-*block*-poly(α,*β*-aspartic acid) diblocks with oppositely charged chicken egg white lysozyme[20,21] and poly(ethylene oxide)-*block*-poly(L-lysine) diblocks.[22] These authors showed that there was a chain length recognition, the supramolecular assembly being the result of the association of the oppositely charged blocks of the same length. Kabanov et al. reported on similar complexes formed by mixing poly(ethylene oxide)-*block*-poly(sodium methacrylate) diblocks and poly(*N*-ethyl-4-vinylpyridinium bromide) polycations.[23] Conversely micellar aggregates should be formed upon mixing a water-soluble polyanion and a diblock copolymer consisting of two water-soluble blocks: one cationic and one neutral. Upon mixing the two components, an IPEC core would be formed and the water-soluble nonionic block would stabilize micelles. In this paper, P2VP-*b*-PEO diblocks will be mixed with $PSSO_3Na$ polyanions. The $PSSO_3Na$ polyanions remain negatively charged in a pH range in which the ionization of the P2VP block can be changed from 0 to 100%. So,

* To whom correspondence should be addressed.
† University of Liège.
‡ J.-F. Gohy is "Chargé de Recherches" by the National Fund for Scientific Research (FNRS).
§ Polymer Source.

10.1021/ma001160y CCC: $19.00
Published on Web 11/23/2000

at low pH, P2VP is protonated, and micelles are expected to be formed with an IPEC core and a corona consisting of PEO blocks and a possible excess of uncomplexed charges. At higher pH, the P2VP blocks will be deprotonated and insoluble in water, so that formation of micelles consisting of a P2VP core surrounded by a PEO corona should be observed. Therefore, the system under consideration has the originality to form two types of aggregates depending on the pH of the aqueous solution. The supramolecular association of P2VP-*b*-PEO/$PSSO_3Na$ mixtures will be studied as a function of pH, $PSSO_3Na$ molecular weight and pyridinium cation/sulfonate anion molar ratio. Light scattering will be the main technique used to characterize the supramolecular assemblies.

Experimental Section

Polymer Synthesis. The diblock copolymer was synthesized by sequential living anionic copolymerization, under argon atmosphere in tetrahydrofuran (THF), with rigorously purified monomers and solvents. Diphenyl methyl potassium was used to initiate the polymerization of 2-vinylpyridine at −78 °C. Then, 30 min later, an aliquot was picked out from the reactor for size exclusion chromatography (SEC). SEC was carried out with a Varian liquid chromatograph equipped with a refractive index detector and calibrated by polystyrene standards. Three columns from Supelco (G6000−4000−2000 HXL) were used with THF added with 2 vol % triethylamine as the eluent. Ethylene oxide was added, and the temperature was raised to 35 °C for 24 h. Polymerization was stopped by addition of methanol, and the P2VP-*b*-PEO copolymer was recovered by precipitation in hexane, followed by drying in vacuo at 40 °C for 48 h. From SEC analysis of the first block, M_n(P2VP) = 4300 and M_w/M_n = 1.15. SEC analysis also showed that the diblock was contaminated by less than 2 wt % of P2VP homopolymer. M_n of the second block was calculated from the copolymer composition (^{1}H NMR analysis) and M_n of the first block. Accordingly, M_n(copolymer) = 13 300 and M_w/M_n = 1.05.

$PSSO_3Na$ homopolymers were standards for SEC purchased from Polyscience (polydispersity smaller than 1.1). They will be designated by the acronym $PSSO_3Na$ (X), where X stands for $M_n \times 10^{-3}$.

Preparation of the Solutions. Aqueous solutions were prepared by direct dissolution of known amounts of solid samples in glass vessels containing pH- and ionic strength-adjusted water. pH was controlled by a 50 mM phosphate buffer. When required, pH was changed by the dropwise addition of 100 mM HCl or NaOH aqueous solution and the pH was monitored by a calibrated potentiometric pH-meter. NaCl was used to adjust the ionic strength, when required. In all the experiments, bidistilled water was used and was filtered through 0.2 μm filters. Different pyridinium cation/sulfonate anion molar ratios (n_{anion}/n_{cation}) were considered.

Light Scattering. Dynamic and static light-scattering measurements were carried out with a Brookhaven Instruments Corp. DLS apparatus that consisted of a BI-200 goniometer, a BI-2030 digital correlator, and an Ar-ion laser (LEXEL Lasers) with a wavelength of 488 nm. A refractive index matching bath of filtered Decalin surrounded the scattering cell, and the temperature was controlled at 25 °C. Prior to sample loading, appropriate glass vessels were soaked overnight in sulfochromic solution, thoroughly cleaned by bidistilled water, and dried in a vacuum oven.

For dynamic light-scattering (DLS) measurements, the scattering angle was 90° and the second-order correlation function $G_2(t)$ was measured. In the case of single-exponential decay, $G_2(t)$ can be expressed by eq 1, where B is the baseline,

$$G_2(t) = B[1 + \beta \exp(-2\Gamma t)] = B[1 + \beta|G_1(t)|^2] \quad (1)$$

β is an optical constant that depends on the instrument, Γ is the decay rate for the process, t is time and $G_1(t)$ is the first-order correlation function. Γ is given by

$$\Gamma = Dq^2 \quad (2)$$

where D is the translation diffusion coefficient, and q is the absolute value of the scattering vector

$$q = [4\pi n \sin(\theta/2)]/\lambda \quad (3)$$

n is the refractive index of the solvent, θ is the diffusion angle and λ is the wavelength of the incident light.

The diffusion coefficient extrapolated to zero concentration (D_0) for spherical particles is related to the hydrodynamic radius, R_h, by the Stokes−Einstein equation

$$D_0 = k_B T/6\pi\eta R_h \quad (4)$$

where k_B is the Boltzmann constant, T is the absolute temperature, and η is the viscosity of the solvent.

When aggregates of different sizes coexist, the experimental correlation function depends on all the individual decay processes and the first-order correlation function is expressed as

$$G_1(t) = \int F(R_h) \exp(-q^2 k_B T t/6\pi\eta R_h)\, dR_h \quad (5)$$

In this case, the R_h distribution is weighted by the intensity $F(R_h)$.

The experimental data were analyzed by the CONTIN routine, a constrained regularization method program for the inverse Laplace transformation of the data, which leads to an optimum $F(R_h)$ size distribution and to best fit of $G_1(t)$ with the data when used in combination with eq 5. The CONTIN program also integrates over each peak in the size distribution and provides a weighted average R_h for each peak. For each sample, the measurements were repeated at least three times.

The polydispersity index of the micellar aggregates was estimated from the μ_2/Γ^2 ratio, in which μ_2 was determined by analysis of the first-order correlation function by the method of the cumulants.

$$G_1(t) = \exp[-\Gamma t + (\mu_2/2)t^2 - (\mu_3/3!)t^3 + ...] \quad (6)$$

In the case of static light scattering (SLS), the light scattered by a polymer solution may be expressed as

$$KC/\Delta R(\theta) = 1/M_w[1 + q^2 R_g^2/3] + 2A_2 C \quad (7)$$

where C is the polymer concentration, $\Delta R(\theta)$ is the difference between the Rayleigh ratios for the solution and the solvent, M_w is the weight-average MW, R_g^2 is the mean square radius of gyration, A_2 is the second virial coefficient and $K = [4\pi^2 n^2 (dn/dc)^2]/(N_A\lambda^4)$ (N_A is the Avogadro number). Toluene of known Rayleigh ratio was used as a calibration standard. The refractive index increment (dn/dc) was measured for each sample by a Optilab DSP interferometric refractometer from Wyatt Technology at λ = 488 nm. Measurements were carried out at angles varying from 30 to 150°. SLS measurements were carried out in pH-adjusted water in order to determine the absolute weight-average MW of the micellar aggregates. The absolute weight-average MW of the nonassociated copolymer chains was measured with an aqueous P2VP-*b*-PEO solution at pH = 3.

Electrophoretic Mobility. A Coulter DELSA 440 was used to measure the electrophoretic mobility. As result of the Doppler effect, the frequency of the scattered laser light is different from the frequency of the original laser beam. This frequency shift is related to the particle velocity. The relationship between the frequency shift and the electrophoretic mobility is expressed by the following equation:

$$U = (\nu_d \lambda)/[2En \sin(\theta/2)] \quad (8)$$

ν_d is the frequency shift, U is the electrophoretic mobility, and E is the electrical field strength.

The ζ potential is related to the electrophoretic mobility by eq 9, where ϵ is the dielectric constant.

$$U = \frac{\epsilon\zeta}{\eta} \tag{9}$$

The ζ potential was measured in 100 mM NaCl solutions in order to keep the electrical double layer constant.

Results and Discussion

The pH-dependent micellization of the protonated P2VP-*b*-PEO copolymer will be first discussed. The supramolecular association of P2VP-*b*-PEO and $PSSO_3$-Na will then be studied by dynamic light scattering in relation to pH. Static light-scattering data will be collected in order to elucidate the structure of the micelles. Finally, dynamic and static light-scattering measurements will be combined with the purpose to clear up the mechanism of IPEC formation in the binary system under consideration.

pH-Dependent Micellization of the P2VP-*b*-PEO Copolymer. The pH-dependent self-association behavior of P2VP-*b*-PEO was previously studied by Webber et al.[14] Because a diblock with a different composition is analyzed in this study its pH-dependent behavior could advantageously complete the available information. The P2VP-*b*-PEO diblock considered in this paper forms monodisperse spherical micelles at pH higher than 6.1, thus, when the P2VP block is essentially uncharged and is a typical hydrophobic block. In contrast to the results previously reported by Webber et al., the micelle size is independent of the copolymer concentration, which confirms that no anomalous micellization phenomenon occurs in the sample under investigation, in agreement with a very low content of residual P2VP homopolymer in the diblock. At lower pH, unimers are observed. This pH-dependent behavior is completely reversible, as assessed by several addition cycles of HCl followed by NaOH to the aqueous copolymer solution. The visual inspection of the copolymer solution shows a transition from a optically clear solution at low pH (unimer solution) to a bluish scattering solution at pH exceeding 6.1 (micellar solution). The onset of micellization was reported at pH = 4.8 by Webber et al.[14] compared to 6.1 in this study. A reasonable explanation for this difference may be found in the different composition of the two diblocks. Assuming that the pK_a of P2VP can be approximated to the pK_a of ethylpyridine (5.9) and is independent of the degree of protonation of P2VP (which is actually an approximation), the classical expression for the pH of a buffered aqueous solution allows one to calculate the molar fraction of the protonated 2VP units at the onset of micellization. Thus, 92 mol % of the 2VP units would be protonated at the onset of micellization of the copolymer studied by Webber et al., compared to 38 mol % in this study. As result of a very asymmetric composition, the P2VP-*b*-PEO copolymer which contains a major water-soluble PEO block requires a lower degree of P2VP protonation for micellization to occur. Another interesting observation has to be found in the titration curve of protonized P2VP-*b*-PEO copolymers, as shown in Figure 1 of ref 14. The onset of micellization is clearly observed as a plateau at the foot of the sharp break in the pH vs volume of NaOH curve. Thus, the pH remains constant although more NaOH is added, which indicates that the neutralization of the ionized 2VP units is perturbed by the micelle formation and that some ionized 2VP units are entrapped in the P2VP cores and resist neutralization.

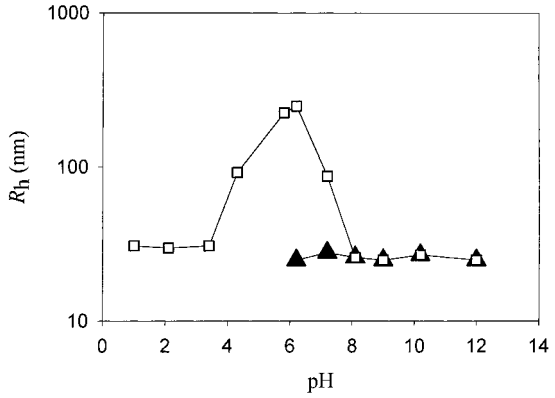

Figure 1. R_h as a function of pH for the P2VP-*b*-PEO (black triangles) and the P2VP-*b*-PEO/$PSSO_3Na$(35.0) complex at $n_{anion}/n_{cation} = 1$ (open squares).

Table 1. DLS and ζ Potential Data for the P2VP-*b*-PEO and P2VP-*b*-PEO/$PSSO_3Na$ Complexes at $n_{anion}/n_{cation} = 1$ and Different pHs (c = 0.1% w/v)

sample	R_h (nm)	μ_2/Γ^2	ζ potential (mV)
	pH = 3		
P2VP-*b*-PEO			
P2VP-*b*-PEO/$PSSO_3Na$(1.8)	28	0.054	0.86 ± 0.48
P2VP-*b*-PEO/$PSSO_3Na$(8.0)	31	0.072	1.2 ± 0.86
P2VP-*b*-PEO/$PSSO_3Na$(35.0)	30	0.060	0.94 ± 0.44
	pH = 9		
P2VP-*b*-PEO	25	0.18	0.76 ± 0.56
P2VP-*b*-PEO/$PSSO_3Na$(1.8)	26	0.21	−0.69 ± 0.47
P2VP-*b*-PEO/$PSSO_3Na$(8.0)	25	0.17	−1.4 ± 0.85
P2VP-*b*-PEO/$PSSO_3Na$(35.0)	27	0.22	−1.2 ± 0.68

The addition of $PSSO_3Na$ polyanion to the aqueous solution of P2VP-*b*-PEO unimers at low pH leads to the electrostatic complexation of the positively charged P2VP blocks and the negatively charged $PSSO_3Na$ chains. These IPEC self-associate in water, the micellar aggregates being stabilized by the nonionic water-soluble block attached to the protonated P2VP blocks. The MW of the $PSSO_3Na$ chains has been changed from 1800 to 35 000. In all cases, bluish scattering micellar solutions are observed, which is the signature of the self-assembly of the interpolyelectrolyte complex formed.

Dynamic Light Scattering of the Micellar Complexes. Figure 1 shows how the hydrodynamic radius (R_h) changes with the pH for the P2VP-*b*-PEO diblock and its water-soluble stoichiometric complex with $PSSO_3$-Na(35.0). The PEO-*b*-P2VP copolymer is dissolved as free chains in water as long as the P2VP block is protonated. At pH > 6.1, micelles with R_h of ca. 25 nm are formed and polydispersity (μ_2/Γ^2) of 0.102. These micelles consist of an essentially uncharged P2VP core surrounded by a PEO corona, in agreement with a very low ζ-potential (Table 1). Figure 2a is a schematic picture of these micelles. The behavior of the PEO-*b*-P2VP/$PSSO_3Na$(35.0) mixture is quite different, and it can be divided into three regions as shown in Figure 1. From pH = 1 to pH = 3.5, micelles are formed with R_h of ca. 30 nm and a very low polydispersity index. In this low pH range, the P2VP block is almost completely protonated and it is complexed by the negatively charged $PSSO_3Na$ chains. According to the scientific literature,[19−23] these electrostatic complexes could form micelles when one of the two oppositely charged blocks

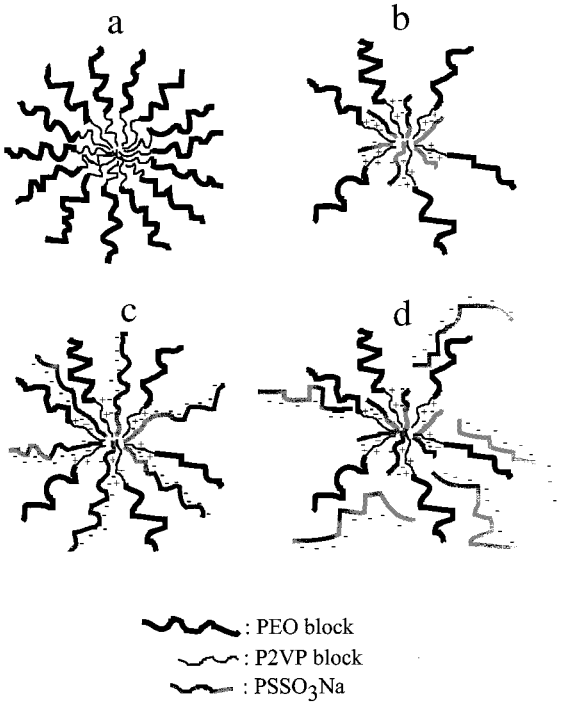

Figure 2. Sketches of micellar structures.

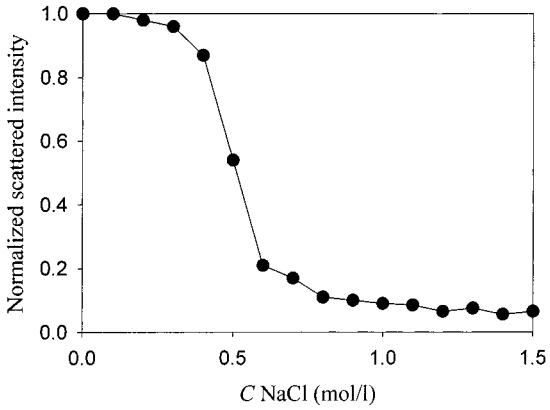

Figure 3. Normalized scattered intensity as a function of NaCl concentration (mol/L) for the P2VP-*b*-PEO/$PSSO_3Na$(35.0) complex at $n_{anion}/n_{cation} = 1$ and pH = 3.

is chemically bonded to a nonionic water-soluble block. The micelles then consist of a core formed by the electrostatic complex surrounded by a corona of the nonionic water-soluble block, as shown in Figure 2b. The very low ζ-potential for the IPEC complexes, n_{anion}/n_{cation} being 1, is also consistent with the stabilization of these micellar aggregates by the PEO blocks (Table 1). That electrostatic interactions are the driving force to micellization is assessed by the effect of the ionic strength on the P2VP-*b*-PEO/$PSSO_3Na$(35.0) complex at pH = 3. Actually, the scattered intensity is sharply decreased, whenever the NaCl concentration exceeds 0.5 mol/L, in complete agreement with results previously reported for similar complexes.[19,23] Furthermore, no micelle can be detected at and above this salt concentration (Figure 3). The second region extends from pH = 3.5 to pH = 7 and is characterized by a low scattered intensity more likely due to lose large size IPEC aggregates. In the third region, the scattered intensity is significantly increased compared to the second region, and micelles with $R_h = 25$ nm and a polydispersity index of 0.11 are detected. These micelles are thought to consist of an

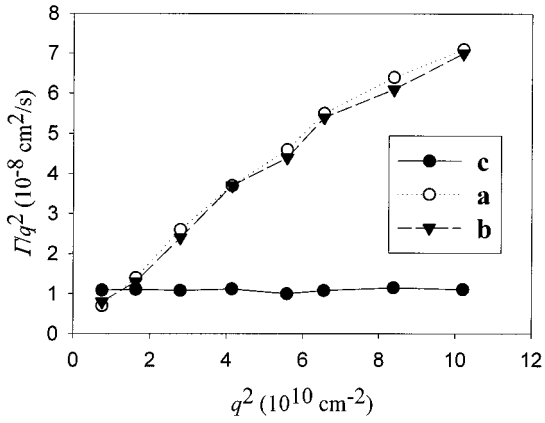

Figure 4. Γ/q^2 as a function of q^2 for the P2VP-*b*-PEO diblock at pH = 9 (a), the P2VP-*b*-PEO/$PSSO_3Na$(35.0) complex at $n_{anion}/n_{cation} = 1$ and pH = 9 (b), and the P2VP-*b*-PEO/$PSSO_3$-Na(35.0) complex at $n_{anion}/n_{cation} = 1$ and pH = 3 (c).

essentially uncharged P2VP core surrounded by a PEO corona, as it was observed for the P2VP-*b*-PEO copolymer at the same pH's. These micelles are not perturbed by salt addition. Similar observations hold for all the P2VP-*b*-PEO/$PSSO_3Na$ mixtures prepared in this study. It must be noted that conventional P2VP-*b*-PEO micelles are formed at pH > 6.1 by the neat diblock compared to pH > 7 in the presence of $PSSO_3Na$. This observation is consistent with the entrapment of ionized 2VP units in the P2VP cores of the conventional micelles, as discussed above. When $PSSO_3Na$ is added, the ionized 2VP units form an IPEC complex with the polyanions, which prevent them from being entrapped in the P2VP cores. Therefore, micelles with P2VP core and PEO corona are observed at a higher pH for the P2VP-*b*-PEO/$PSSO_3Na$ mixture than for the neat P2VP-*b*-PEO copolymer.

On the basis of these experimental observations, the association behavior of the P2VP-*b*-PEO/$PSSO_3Na$ mixtures can be rationalized as follows: at pH < 3.5, micelles are formed with a core consisting of electrostatic complexes between positively charged P2VP and $PSSO_3Na$; at 3.5 < pH < 7, these micelles are no longer stable as result of the rapid decrease of the positive charge density on P2VP upon increasing pH and loose large size aggregates persist; at pH > 7, the P2VP blocks are essentially uncharged and trigger the formation of micelles which coexist with free $PSSO_3Na$ chains.

The micelles formed at $n_{anion}/n_{cation} = 1$ have been characterized by a DLS analysis based on a cumulant approach. Figure 4 shows the dependence of the diffusion coefficient on the detection angle. In this respect, Γ/q^2 has been plotted against q^2. For spherical particules, the rotational motion is not detectable, and Γ/q^2 is independent of q^2.[24] This situation is clearly observed for the P2VP-*b*-PEO/$PSSO_3Na$(35.0) complex at pH = 3. In sharp contrast, essentially the same linear increase of Γ/q^2 with q^2 is observed for both the P2VP-*b*-PEO and the P2VP-*b*-PEO/$PSSO_3Na$(35.0) mixture at pH = 9, which suggests that these samples form nonspherical micelles of similar shape.

The effect of the MW of the $PSSO_3Na$ polyanion on the characteristic features of the IPEC micelles has also been examined at pH = 3. The results are shown in Table 1 for $n_{anion}/n_{cation} = 1$. The small variations in R_h and μ_2/Γ^2 cannot be accounted for by a change in the micellar structure upon complexation with $PSSO_3Na$ of different MW. Thus, the characteristic features of the

Table 2. SLS Data Obtained for the P2VP-*b*-PEO Diblock and the P2VP-*b*-PEO/$PSSO_3Na$(35.0) Complex at n_{anion}/n_{cation} = 1and Different pHs

sample	$M_w \times 10^{-6}$	Z	R_g (nm)	R_g/R_h	V_0/V
	pH = 3				
P2VP-*b*-PEO	0.0156	1	6.8	1.7	
P2VP-*b*-PEO/$PSSO_3Na$(35.0)	2.35	98	21.3	0.71	0.035
	pH = 9				
P2VP-*b*-PEO	3.85	247	60	2.4	0.098
P2VP-*b*-PEO/$PSSO_3Na$(35.0)	3.96	254	63.4	2.35	0.10

IPEC micelles basically depend on the diblock used, at least in the investigated $PSSO_3Na$ MW range.

Static Light Scattering (SLS) of the Micellar Complexes. The absolute weight-average molar mass, $M_{w,micelle}$, can be calculated from SLS experiments. This value allows the aggregation number (Z) of the micelles to be known since $Z = M_{w,micelle}/M_{w,copolymer}$, where $M_{w,copolymer}$ is the weight-average molar mass of the single diblock copolymer molecule. The aggregation number has been determined for the P2VP-*b*-PEO block copolymer at pH = 9 and for the P2VP-*b*-PEO/$PSSO_3$-Na(35.0) mixture at pH = 3 and pH = 9 (Table 2), with $n_{anion}/n_{cation} = 1$. The aggregation number is essentially the same for the P2VP-*b*-PEO/$PSSO_3Na$ mixture and the P2VP-*b*-PEO diblock at pH = 9. This observation is in agreement with the DLS data, R_h and the polydispersity index being indeed identical for these two systems. For the P2VP-*b*-PEO/$PSSO_3Na$(35.0) complex at pH = 3, Z has been calculated from the relationship $Z = M_{w,micelle}/(M_{w,copolymer} + AM_{w,PSSO3Na})$, where $M_{w,PSSO3Na}$ is the weight-average molecular weight of the $PSSO_3Na$ polyanion and A is a proportionality factor related to the stoichiometry of the P2VP-*b*-PEO/$PSSO_3Na$(35.0) complex. In this case, Z represents the number of P2VP-*b*-PEO/$PSSO_3Na$(35.0) IPEC that self-assembles to form a micelle.

SLS also makes the z-average radius of gyration, R_g, available. The R_g/R_h ratio gives valuable information on the architecture of the particles.[25] Because R_h determined from the first cumulant is also a z-average, these data can be directly compared. Table 2 shows that $R_g/R_h < 1$ for the P2VP-*b*-PEO/$PSSO_3Na$(35.0) complex with $n_{anion}/n_{cation} = 1$ at pH = 3. This value is consistent with micelles or aggregates with a dense nucleus and with homogeneous spheres or hollow spheres (vesicles). It definitely does not fit coiled molecules ($R_g/R_h = 1.8$) and rods ($R_g/R_h > 2$). The R_g/R_h ratio of 0.71 is also close to the theoretical value (0.776) for a hard sphere.[26] This similarity was reported elsewhere for water-soluble IPEC complexes.[20] The smaller experimental value compared to the theoretical one may reflect a change in the segmental density along the radial direction. Moreover, it must be noted that $R_g/R_h = 0.707$[27] has been calculated for a star-shaped macromolecule with no central core and is thus very close to the value observed for this sample. So a starlike micelle model with a small condensed core surrounded by expanded PEO chains could fit the experimental results. If the PEO chains are twisted into expanded helical coils, the end-to-end distance should be 36.7 nm for PEO with a degree of polymerization of 204 (MW = 9000).[28] Another extreme conformation for stretched PEO chain is a zigzag conformation, where the end-to-end distance should be 71.4 nm (MW = 9000).[28] Furthermore, a value of 4.3 nm has been calculated for the end-to-end distance of PEO (MW = 9000) with a random coil conformation.[28]

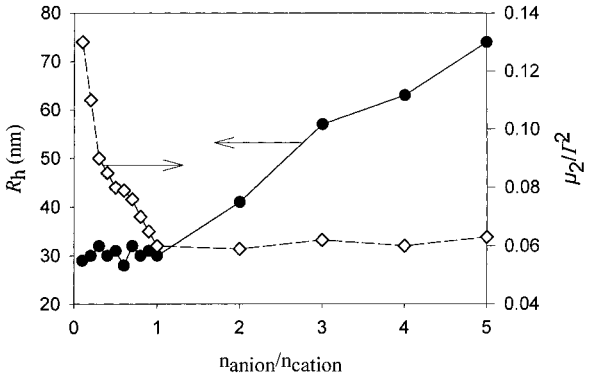

Figure 5. R_h (black dots) and μ_2/Γ^2 (open squares) for the P2VP-*b*-PEO/$PSSO_3Na$(35.0) complex as a function of the n_{anion}/n_{cation} stoichiometric ratio at pH = 3.

The experimental value of R_h in Table 1 suggests that PEO chains in the micelles are not fully extended, which agrees with results reported for other block copolymer micelles of a core−shell architecture.[29] In sharp contrast, $R_g/R_h > 2$ for the P2VP-*b*-PEO and for the P2VP-*b*-PEO/$PSSO_3Na$(35.0) mixture at pH = 9. Therefore, rodlike micelles are expected to be formed in these two cases. Because the P2VP-*b*-PEO/$PSSO_3Na$(35.0) mixture at pH = 9 consists of a mixture of P2VP-*b*-PEO micelles and $PSSO_3Na$ free chains, it is not surprising that the characteristic features of the micelles are nearly the same for the P2VP-*b*-PEO/$PSSO_3Na$(35.0) mixture and the P2VP-*b*-PEO copolymer at pH = 9.

From R_h (from DLS) and M_w (from SLS), the average packing density, V_0/V, of the micellar particles can be estimated.[25] The particles are assumed to be spheres of diameter $2R_h$ and hydrodynamic volume $V = {}^4/_3\pi R_h^3$. These values have to be compared with the volume V_0 of the same amount of bulk polymer. A polymer density of 1 has been assumed in the calculations. The relative packing density lies between 0 and 1. Alternatively, the degree of swelling can be defined as $s = V/V_0 - 1$. Table 2 shows that the packing density is 10% for the P2VP-*b*-PEO copolymer and the P2VP-*b*-PEO/$PSSO_3Na$(35.0) mixture at pH = 9, compared to only 3.5% for the P2VP-*b*-PEO/$PSSO_3Na$(35.0) complex at pH = 3. As a reference, a polymer latex has a packing density of ca. 1, whereas a randomly coiled linear macromolecule has a density smaller than 1%.[25] Although, these data may not be directly compared, because the P2VP-*b*-PEO and the P2VP-*b*-PEO/$PSSO_3Na$(35.0) mixture at pH = 9 do not form spherical micelles, the hydrophilic chains in the corona are much extended in the P2VP-*b*-PEO/$PSSO_3Na$(35.0) complex at pH = 3, consistent with a starlike model.

Cooperative Association Mechanism for the Complexation of P2VP-*b*-PEO and $PSSO_3Na$. The association mechanism of protonated P2VP-*b*-PEO with $PSSO_3Na$ has been investigated at pH = 3 by changing the n_{anion}/n_{cation} molar ratio from 0.1 to 5.0 and analyzing the complexes by DLS. Figure 5 shows that R_h remains constant (at ca. 30 nm) and the polydispersity index decreases from 0.13 to 0.06 in the $0.1 \leq n_{anion}/n_{cation} \leq 1.0$ range. R_h increases linearly from 30 to 75 nm whereas the polydispersity remains constant at an extremely low value of 0.06 when the n_{anion}/n_{cation} ratio is increased from 1.0 to 5.0. So, whatever the characteristic feature under consideration, Figure 5 emphasizes two regions with a boundary at $n_{anion}/n_{cation} = 1.0$. Although the polydispersity index is relatively small in

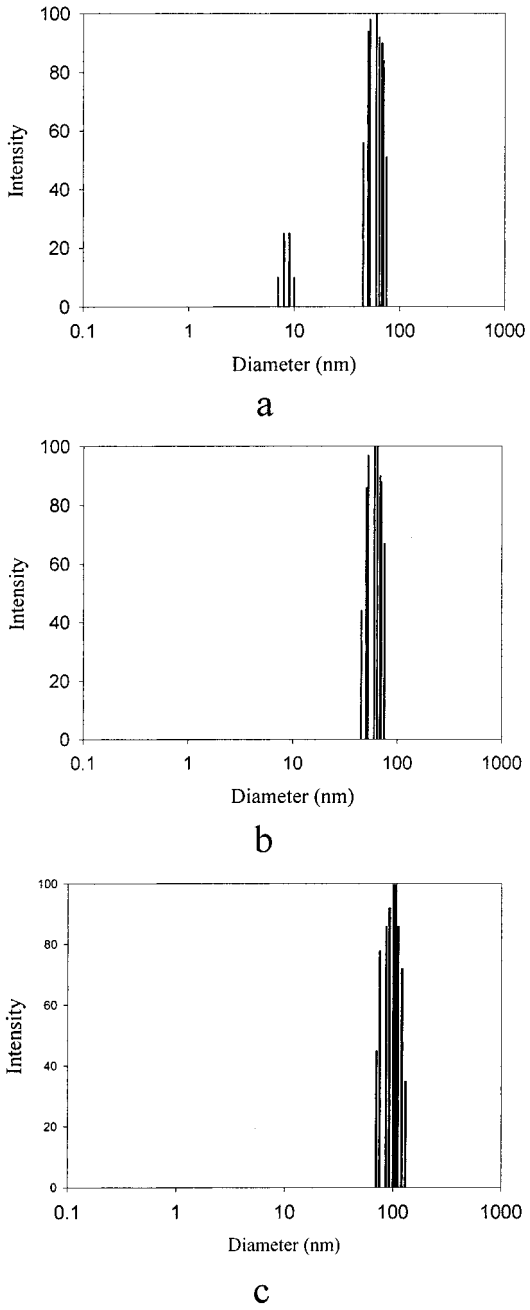

Figure 6. CONTIN size distribution of the P2VP-*b*-PEO/$PSSO_3Na$ (35.0) IPEC at pH = 3 and n_{anion}/n_{cation} = 0.2 (a), n_{anion}/n_{cation} = 1 (b) and n_{anion}/n_{cation} = 3 (c), respectively.

the $0.1 \leq n_{anion}/n_{cation} \leq 1.0$ range, it decreases by a factor of 2 when the n_{anion}/n_{cation} molar ratio is increased up to 1.0. In parallel, the CONTIN analysis of the DLS data shows a bimodal distribution at $n_{anion}/n_{cation} = 0.2$ (Figure 6). A minor fraction with a small R_h (4 nm) is observed in addition to the main population at $R_h = 30$ nm. At $n_{anion}/n_{cation} = 1.0$, the distribution becomes monomodal with an average R_h of 30 nm. It is worth noting that the major fraction in the CONTIN histogram has a constant $R_h = 30$ nm regardless of the n_{anion}/n_{cation} molar ratio in this region. The small-size fraction in the CONTIN histogram of Figure 6 has been attributed to the uncomplexed P2VP-*b*-PEO copolymer chains. These results agree with a cooperative association mechanism of P2VP-*b*-PEO and $PSSO_3Na$. So, the system would consist of IPEC and free P2VP-*b*-PEO chains when n_{anion}/n_{cation} is smaller than 1.0, while only IPEC is

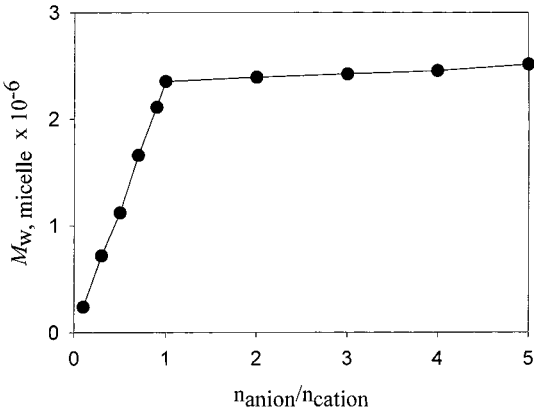

Figure 7. $M_{w,micelles}$ as a function of the n_{anion}/n_{cation} molar ratio for the P2VP-*b*-PEO/$PSSO_3Na$(35.0) complex at pH = 3.

observed at $n_{anion}/n_{cation} = 1.0$. A cooperative association mechanism is also in line with the monotonic decrease of the polydispersity index in the $0.1 < n_{anion}/n_{cation} < 1.0$ range.

The cooperative association at $n_{anion}/n_{cation} \leq 1.0$ is also supported by the SLS data. In this respect, M_w of the micellar aggregates, calculated by eq 7 has been plotted as a function of the n_{anion}/n_{cation} molar ratio (Figure 7). As it was observed for the DLS data, Figure 7 shows two regions with a boundary at $n_{anion}/n_{cation} = 1.0$. The M_w of the micelles linearly increases whenever this molar ratio is increased up to 1.0. At higher n_{anion}/n_{cation} ratios, the slope of the linear dependence is substantially decreased. According to Kataoka et al., this behavior is the signature of a cooperative association mechanism.[20] Similar observations have been reported for the complexation of lysozymes with various anionic polyelectrolytes, for which a cooperative precipitation occurs.[30−32]

When $n_{anion}/n_{cation} > 1.0$, the size of the micelles increases and the polydispersity index remains very small and constant. The CONTIN analysis of the DLS data shows only one micelle population (Figure 6). Therefore, whenever the $PSSO_3Na$ polyanions are in excess with respect to the protonated P2VP-*b*-PEO copolymer, IPEC are formed that contain uncomplexed $PSSO_3Na$ chain segments. All the $PSSO_3Na$ chains are part of micellar aggregates, no free $PSSO_3Na$ chains being detected in solution at least within the limits of the DLS analysis. All these observations are very similar to the ones previously reported by Kataoka et al. for the complexation of lysozymes by poly(ethylene oxide)-*block*-poly(aspartic acid) diblocks,[20,21] with the sharp difference that the anionic groups are part of a diblock in this previously reported work. Moreover, Kataoka et al. observed a mixture of IPEC micelles and free cationic lysozymes "homopolymer" for $n_{anion}/n_{cation} < 1.0$. In the present study, $PSSO_3Na$ homopolymers are never detected as free chains. Figure 2 interestingly compares the structures proposed for the micellar aggregates observed in this study. Figure 2a refers to the structure of the "classic micelles" formed by the P2VP-*b*-PEO copolymer or the P2VP-*b*-PEO/$PSSO_3Na$ mixture at pH > 6.1, which consist of a hydrophobic nonprotonated P2VP core surrounded by a PEO corona. The structure of the IPEC micellar aggregates formed at pH < 3.5 by the P2VP-*b*-PEO/$PSSO_3Na$ complex is shown in Figure 2b, when $0.1 \leq n_{anion}/n_{cation} \leq 1.0$ and in Figure 2c when n_{anion}/n_{cation} exceeds 1.0. Actually, the uncomplexed $PSSO_3Na$ chain segments in Figure 2c are intermingled in the PEO corona and contribute to the

Table 3. ζ Potential for the P2VP-*b*-PEO/$PSSO_3Na$(35.0) Complex at pH = 3, at different n_{anion}/n_{cation} Molar Ratios (c = 0.1% w/v)

n_{anion}/n_{cation}	ζ potential (mV)
0.2	0.88 ± 0.34
0.5	0.96 ± 0.56
1	0.94 ± 0.44
2	−5.86 ± 1.3
3	−12.6 ± 1.7
5	−21.8 ± 2.4

micelle stabilization by an electrosteric mechanism. This structural feature is confirmed by the ζ-potential measured in the $n_{anion}/n_{cation} > 1.0$ region (Table 3). Indeed, the ζ-potential is very small in the $1 \leq n_{anion}/n_{cation} \leq 1.0$ range in agreement with micelles essentially stabilized by the nonionic PEO blocks. Whenever n_{anion}/n_{cation} is higher than 1.0, a negative ζ potential increases sharply, in agreement with the contribution of $PSSO_3Na$ chain segments to the corona, as schematized in Figure 2c. This model can also account for the increased size of the micelles at $n_{anion}/n_{cation} > 1.0$, because the increasing density of the negatively charged species in the micelle corona is responsible for electrostatic repulsion and stretching of the corona.

The observations at $n_{anion}/n_{cation} > 1.0$ and the scheme shown in Figure 2c are in apparent contradiction with a cooperative mechanism. Indeed, although P2VP-*b*-PEO/$PSSO_3Na$ IPEC of well-defined MW and nonassociated $PSSO_3Na$ chains are expected to coexist, no free $PSSO_3Na$ chains are observed at least within the experimental limit of detection. This conclusion could however result from the adsorption of the excess of $PSSO_3Na$ chains onto the well-defined P2VP-*b*-PEO/$PSSO_3Na$ complex formed by the cooperative association mechanism. If it were so, the model of Figure 2c should be revised in favor of the model shown in Figure 2d. Moreover, the model of Figure 2c cannot be excluded on the basis of the increase in R_h as $n_{anion}/n_{cation} > 1.0$ (see Figure 5), since R_h is expected to increase in both models in Figure 2c and Figure 2d when an excess of $PSSO_3Na$ chains is added.

To clear up this situation, additional DLS experiments have been carried out. If the model of Figure 2c is valid, further addition of protonated P2VP-*b*-PEO copolymer is expected to increase the size of the IPEC core (see Figure 8a) since all the $PSSO_3Na$ chains are already entrapped in IPEC micelles. In the case of a cooperative association mechanism, addition of protonated P2VP-*b*-PEO to micelles of the type in Figure 2d should result in the desorption of the $PSSO_3Na$ chains and thus in a larger number of smaller micelles, as schematized in Figure 8b. Figure 9 shows how R_h and the scattered intensity for the P2VP-*b*-PEO/$PSSO_3Na$-(35.0) IPEC with $n_{anion}/n_{cation} = 2$ changes when various amounts of the protonated P2VP-*b*-PEO copolymer are added. This figure is nothing but the mirror image of Figure 5. A decrease in the size of the micelles is observed as the n_{anion}/n_{cation} ratio is decreased. A plateau is reached at $n_{anion}/n_{cation} \leq 1$, and a value of 30 nm is noted for R_h, in agreement with the cooperative association mechanism previously discussed. The increase in the scattered intensity in the $1 < n_{anion}/n_{cation} < 2$ range can be accounted for by the increasing number of micelles. These experimental results clearly show that the model of Figure 2c should be rejected in favor of the model of Figure 2d.

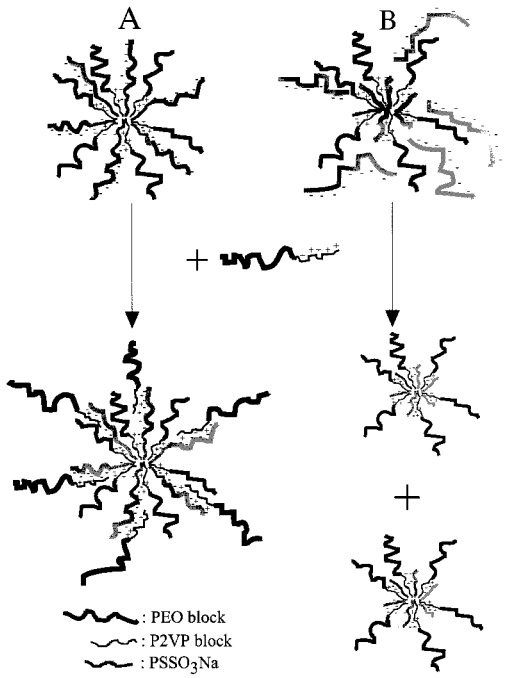

Figure 8. Sketches of micellar structures when protonated P2VP-*b*-PEO diblock is added to micelles of type 2c (A) and 2d (B) (see Figure 2).

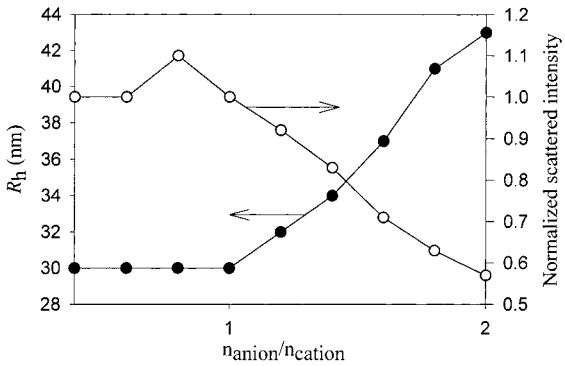

Figure 9. R_h and normalized scattered intensity as a function of the n_{anion}/n_{cation} molar ratio. This ratio is changed by the addition of protonated P2VP-*b*-PEO to the P2VP-*b*-PEO/$PSSO_3Na$ (35.0) IPEC at pH = 3 with $n_{anion}/n_{cation} = 2$.

Conclusions

In this paper, water-soluble complexes have been prepared by mixing a P2VP-*b*-PEO diblock with $PSSO_3Na$ polyanions at low pH. These complexes form well-defined, spherical micelles that consist of a dense core of IPEC formed by the protonated P2VP and $PSSO_3Na$ chains, surrounded by a corona of PEO. The morphological features of these micelles mainly depend on the P2VP-*b*-PEO diblock, whatever the $PSSO_3Na$ MW, whereas their stability is strongly pH-dependent. Indeed, at high pH, the P2VP blocks are essentially nonprotonated and thus hydrophobic, so releasing the pH-insensitive $PSSO_3Na$ polyanions in solution. The hydrophobic nonprotonated P2VP blocks then aggregate to form the core of rodlike micelles stabilized by the PEO blocks. These micelles are identical to the ones formed whenever neat P2VP-*b*-PEO diblock is dissolved in water at high pH.

The formation of these two types of micelles is reversible, change in the solution pH making the system to oscillate between the two extreme situations. More-

over, no change in the micelle characteristic features has been detected so far after several cycles of pH variation.

Finally, a cooperative association mechanism has been emphasized for the formation of IPEC at low pH.

Acknowledgment. J.F.G., S.A., and R.J. are very much indebted to the "Services Fédéraux des Affaires Scientifiques, Techniques et Culturelles" for financial support in the frame of the "Pôles d'attraction Interuniversitaires: 4-11: Chimie Supramoléculaire et Catalyse Supramoléculaire". J.F.G. and R.J. are grateful to M. Dejeneffe (CERM, Liège) for her technical assistance.

References and Notes

(1) Creutz, S.; Jérôme, R.; Kaptijn, G. M. P.; van der Wert, A. W.; Akkerman, J. M. *J. Coat. Technol.* **1998**, *70*, 41.
(2) Yokoyama, M.; Okano, T.; Sakurai, Y.; Ekimoto, H.; Shibazaki, C.; Kataoka, K. *Cancer Res.* **1991**, *51*, 3229.
(3) Förster, S.; Zizenis, M.; Wenz, E.; Antonietti, M. *J. Chem. Phys.* **1996**, *104*, 9956.
(4) See, for example: Moffit, M.; Khougaz, K.; Eisenberg, A. *Acc. Chem. Res.* **1996**, *29*, 95.
(5) (a) Zhang, L.; Eisenberg, A. *J. Am. Chem. Soc.* **1996**, *118*, 3168. (b) Zhang, L.; Eisenberg, A. *Science* **1995**, *268*, 1728.
(6) Ding, J.; Liu, G. *Macromolecules* **1997**, *30*, 655.
(7) Cornelissen, J. J.; Fischer, M.; Sommerdijk, N. A.; Nolte, R. J. *Science* **1998**, *280*, 1427.
(8) Discher, B. M.; Won, Y. Y.; Ege, D. S.; Lee, J. C. M.; Bates, F. S.; Discher, D. E.; Hammer, D. A. *Science* **1999**, *284*, 1143.
(9) Yu, K.; Eisenberg, A. *Macromolecules* **1998**, *31*, 3509.
(10) Gohy, J.-F.; Creutz, S.; Garcia, M.; Mahltig, B.; Stamm, M.; Jérôme, R. *Macromolecules* **2000**, *33*, 6378.
(11) Selb, J.; Gallot, Y. In *Developments in Block Copolymers*; Goodman, I., Ed.; Elsevier: Amsterdam, 1985; Vol. 2, p 85.
(12) Bütün, V.; Billingham, N. C.; Armes, S. P. *Chem. Commun.* **1997**, 671.
(13) Rahman, A.; Brown, C. W. *J. Appl. Polym. Sci.* **1983**, *28*, 1331.
(14) Martin, T. J.; Prochakza, K.; Munk, P.; Webber, S. E. *Macromolecules* **1996**, *29*, 6071.
(15) Lee, A. S.; Gast, A.; Bütün, V.; Armes, S. P. *Macromolecules* **1999**, *32*, 4302.
(16) Kabanov, V. A. *Pure Appl. Chem. Macromol. Chem.* **1973**, *8*, 121.
(17) Tsuchida, E.; Abe, K. *Adv. Polym. Sci.* **1982**, *45*, 2.
(18) Kabanov, V. A.; Zezin, A. B. *Makromol. Chem. Suppl.* **1985**, *13*, 137.
(19) Cohen Stuart, M. A.; Besseling, N. A. M.; Fokkink, R. G. *Langmuir* **1998**, *14*, 6846.
(20) Harada, A.; Kataoka, K. *Macromolecules* **1998**, *31*, 288.
(21) Harada, A.; Kataoka, K.*Langmuir* **1999**, *15*, 4208.
(22) Harada, A.; Kataoka, K. *Science* **1999**, *283*, 65.
(23) Kabanov, A. V.; Bronich, T. K.; Kabanov, V. A.; Yu, K.; Eisenberg, A. *Macromolecules* **1996**, *29*, 6797.
(24) Xu, R.; Winnik, M. A.; Hallett, F. R.; Riess, G.; Croucher, M. D. *Macromolecules* **1991**, *24*, 87.
(25) Schuch, M.; Kingler, J.; Rossmanith, P.; Frechen, T.; Gerst, M.; Feldthusen, J.; Müller, A. H. E. *Macromolecules* **2000**, *33*, 1734.
(26) Douglas, J. K.; Roovers, J.; Freed, K. F. *Macromolecules* **1990**, *23*, 4168.
(27) Vagberg, L. J. M.; Cogan, K. A.; Gast, A. P. *Macromolecules* **1991**, *24*, 1670.
(28) Tanford, C.; Nozaki, Y.; Rhode, M. F. *J. Phys. Chem.* **1977**, *81*, 1555.
(29) Astafieva, I.; Khougaz, K.; Eisenberg, A. *Macromolecules* **1995**, *28*, 7127.
(30) Tsuboi, A.; Izumi, T.; Hirata, M.; Xia, J.; Dubin, P. L.; Kokufuta, E. *Langmuir* **1996**, *12*, 6295.
(31) Chen, W.; Berg, J. C. *Chem. Eng. Sci.* **1993**, *48*, 1775.
(32) Clark, K. M.; Glatz, C. E. *Chem. Eng. Sci.* **1992**, *47*, 215.

MA001160Y